International Journal of Engineering & Technology, 9 (1) (2020) 17-25

International Journal of Engineering & Technology

Website: www.sciencepubco.com/index.php/IJET

Research paper

Dynamic modeling and simulation of 10hp induction motor driving a variable load

Oti Stephen Ejiofor [1], Eya Candidus [1], Agada Stephen [2], Uche Ogbuefi [1] *, Ugwuja Peter [1]

[1] *Department of Electrical Engineering, University of Nigeria, Nsukka, Enugu State. Nigeria*
[2] *Dept. of Electrical/Electronic Engineering, Fed. University of Agriculture, Umudike, Abia State. Nigeria*

**Corresponding author E-mail: uche.ogbuefi@unn.edu.ng*

Abstract

This work presents ideally the behavioral characteristics of induction motor (IM) when subjected to different loading conditions. The task is achieved via mathematical modeling of the process using the Simulink tool of the Matlab. Dynamic model is generally used to study the steady state and transient behavior of induction motor. Here, Clarke and Park's transformation of stator and rotor parameters on the synchronously rotating reference frame is applied to the developed mathematical model of the induction motor. First, the differential equations of voltages, currents and flux linkages between the stationary stator and rotating rotor are developed, followed by the mechanical equation of torque and speed. Thereafter the mathematical model developed with the help of the software is generally used to study the variation in parameters value on the dynamic performance of the induction motor as variable load is driven. The obtained simulated results apart from the exhibited performances still suggests that the synchronously rotating reference frame theory is actually a shrewd process to validate the dynamic behavior of the induction motor.

Keywords: *Induction Motor; Performance; Induction; Driving Load; Torque.*

1. Introduction

It is now common to say that asynchronous machines are the work-horse of the modern industry because of their simplicity, rugged construction, reliability, low cost, high efficiency and good self-starting capability [1- 3]. In recent years the control of high-performance induction motor drives for general industrial applications and production automation has received widespread research interests. In an electric drive system the machine is a part of the control system elements. To be able to control the dynamics of the drive system, dynamic behavior of the machine need to be considered. The dynamic behavior of induction motor can be described using dynamic model of the induction motor [4].

The voltage and speed equations that describe the dynamic behavior of an induction motor are time-varying. Therefore, a change of variables can be used to reduce the complexity of these time-varying parameters by eliminating all time-varying inductances, due to electric circuit in relative motion, from the voltage equations of the machine. By this approach, a poly phase winding can be reduced to a set of two phase windings (d-q) with their magnetic axes formed in quadrature. In other words, the stator and rotor variable: voltages, currents and flux linkages, of an induction machine are transferred to a reference frame, which may rotate at any angular velocity or remain stationary. Such reference frame includes:

i) Rotor reference frame ($\omega e = \omega r$): In this frame, the d-q axes rotate at rotor speed and is used when both the stator and rotor voltages are unbalance or discontinuous.
ii) Stationary reference frame ($\omega e = 0$): In this frame, the d-q axes do not rotate and is used when the stator voltages are unbalanced or discontinuous and the rotor voltages are blanched or continuous.
iii) Synchronously rotating reference frame ($\omega e = \omega b$): In this frame, the d-q axes rotates at synchronous speed and it is used when both the stator and rotor voltages are balanced and continuous [5-9]. In [10], the computer simulation for the operating conditions was obtained from the non-linear differential system of equations which describe the symmetrical Induction machine in the stationary reference frame. Here in, the synchronously rotating reference frame is rather used in this work with the following assumptions:

i) The slotting in the stator and rotor produces negligible variation in respective inductances.
ii) Mutual inductances are equal.
iii) Each stator winding is distributed so as to produce a sinusoidal mmf along air gap i.e. space harmonics are negligible.
iv) Saturation, hysteresis and eddy current effects are negligible [11].

It should be noted that variable load machine encompasses the pumps which belong to the class, the torque of which changes as a function of speed. They develop a reduced torque when driven at speeds well below the rated level and an increased torque as the speed grows. The properties of the pump as a motor load are often discussed from the viewpoint of the drive design as well as the pump start-up behavior, response to pump overload, and losses of priming fluid as well as their characteristics as the control system elements [12-15].

2. Dynamic model of the induction motor

The induction machine in d-q or dynamic equivalent circuit is shown below:

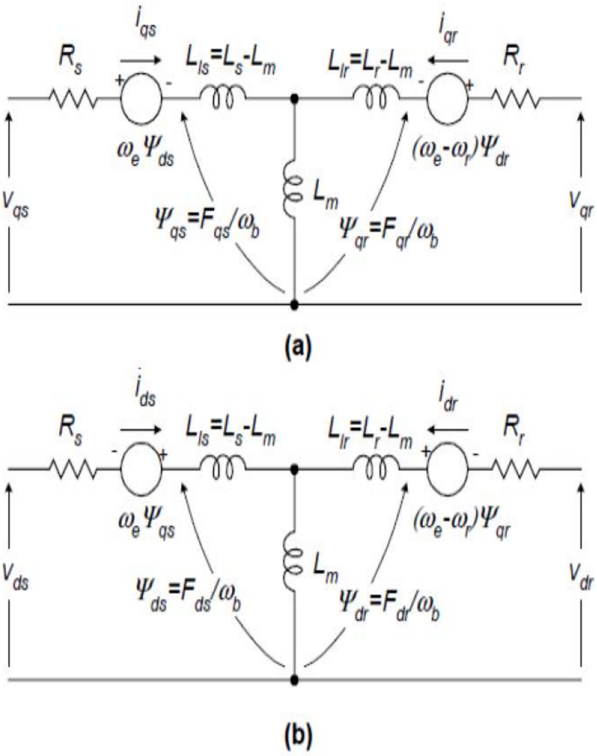

Fig. 1: Dynamic Equivalent Circuits [16], (A) Q-Axis Base (B) D-Axis Base.

From the above dynamic equivalent circuits, the modeling equations in flux linkage form are as follows:

$$\frac{dFqs}{dt} = \omega b\left[Vqs - \frac{\omega e}{\omega b}Fds + \frac{Rs}{Xls}(Fmq - Fqs)\right] \quad (1)$$

$$\frac{dFds}{dt} = \omega b\left[Vds - \frac{\omega e}{\omega b}Fqs + \frac{Rs}{Xls}(Fmd - Fds)\right] \quad (2)$$

$$\frac{dFqr}{dt} = \omega b\left[Vqr - \frac{\omega e - \omega r}{\omega b}Fdr + \frac{Rr}{Xlr}(Fmq - Fqr)\right] \quad (3)$$

$$\frac{dFdr}{dt} = \omega b\left[Vdr + \frac{\omega e - \omega r}{\omega b}Fqr + \frac{Rr}{Xlr}(Fmd - Fdr)\right] \quad (4)$$

For a squirrel cage induction motor as used in this work, Vqr and Vdr are set to zero since the rotor bars shorted. Therefore, the modeling equations of a squirrel cage induction motor become:

$$\frac{dFqs}{dt} = \omega b\left[Vqs - \frac{\omega e}{\omega b}Fds + \frac{Rs}{Xls}(Fmq - Fqs)\right] \quad (5)$$

$$\frac{dFds}{dt} = \omega b\left[Vds - \frac{\omega e}{\omega b}Fqs + \frac{Rs}{Xls}(Fmd - Fds)\right] \quad (6)$$

$$\frac{dFqr}{dt} = \omega b\left[-\frac{\omega e - \omega r}{\omega b}Fdr + \frac{Rr}{Xlr}(Fmq - Fqr)\right] \quad (7)$$

$$\frac{dFdr}{dt} = \omega b\left[\frac{\omega e - \omega r}{\omega b}Fqr + \frac{Rr}{Xlr}(Fmd - Fdr)\right] \quad (8)$$

$$Fmq = Xm1\left[\frac{Fqs}{Xls}+\frac{Fqr}{Xlr}\right] \tag{9}$$

$$Fmd = Xm1\left[\frac{Fds}{Xls}+\frac{Fdr}{Xlr}\right] \tag{10}$$

Where:

$$Xm1 = \left(\frac{1}{Xm}+\frac{1}{Xls}+\frac{1}{Xlr}\right)^{-1}$$

The currents in the d-q axes are given as:

$$Iqs = \frac{1}{Xls}(Fqs - Fmq) \tag{11}$$

$$Ids = \frac{1}{Xls}(Fds - Fmd) \tag{12}$$

$$Iqr = \frac{1}{Xlr}(Fqr - Fmq) \tag{13}$$

$$Idr = \frac{1}{Xlr}(Fds - Fmd) \tag{14}$$

Based on the above equations, the torque and rotor speed can be determined as follows:

$$Te = \frac{2}{3}\frac{p}{2}\frac{1}{\omega b}(FdsIqs - FqsIds) \tag{15}$$

$$\frac{d\omega r}{dt} = \frac{p}{2J}(Te - Tl) \tag{16}$$

The three-phase stator voltages of the induction motor under balanced conditions can be expressed as:

$$Vas = \sqrt{2Vrms}Sin(\omega t) \tag{17}$$

$$Vbs = \sqrt{2Vrms}Sin\left(\omega t - \frac{2\pi}{3}\right) \tag{18}$$

$$Vcs = \sqrt{2Vrms}Sin\left(\omega t + \frac{2\pi}{3}\right) \tag{19}$$

These three-phase voltages are transferred to a synchronously rotating reference frame in only d-q axis transformation (two-phase) using the following two equations.

$$\begin{bmatrix} V\alpha \\ V\beta \end{bmatrix} = \frac{2}{3}\begin{bmatrix} 1 & \frac{1}{2} & -\frac{1}{2} \\ 0 & \frac{\sqrt{3}}{2} & -\frac{\sqrt{3}}{2} \end{bmatrix}\begin{bmatrix} Vas \\ Vbs \\ Vcs \end{bmatrix} \tag{20}$$

$$\begin{bmatrix} Vds \\ Vqs \end{bmatrix} = \begin{bmatrix} cos\theta & -sin\theta \\ sin\theta & cos\theta \end{bmatrix}\begin{bmatrix} V\alpha \\ V\beta \end{bmatrix} \tag{21}$$

The instantaneous values of the stator and rotor currents in the three-phase system are calculated using the following transformation formulae [6-8].

$$\begin{bmatrix} I\alpha \\ I\beta \end{bmatrix} = \begin{bmatrix} cos\theta & -sin\theta \\ sin\theta & cos\theta \end{bmatrix}\begin{bmatrix} Ids \\ Iqs \end{bmatrix} \tag{22}$$

$$\begin{bmatrix} Iai \\ Ibi \\ Ici \end{bmatrix} = \begin{bmatrix} 1 & 0 \\ -\frac{1}{2} & -\frac{\sqrt{3}}{2} \\ -\frac{1}{2} & \frac{\sqrt{3}}{2} \end{bmatrix}\begin{bmatrix} I\alpha \\ I\beta \end{bmatrix} \tag{23}$$

Where i, represents s for stator and r for rotor.

3. MATLAB/Simulink implementation

The three-phase induction motor model is implemented using the same sets of equations derived above and simulated using the Matlab/Simulink. Figure2 below shows the complete Simulink model of the required induction motor.

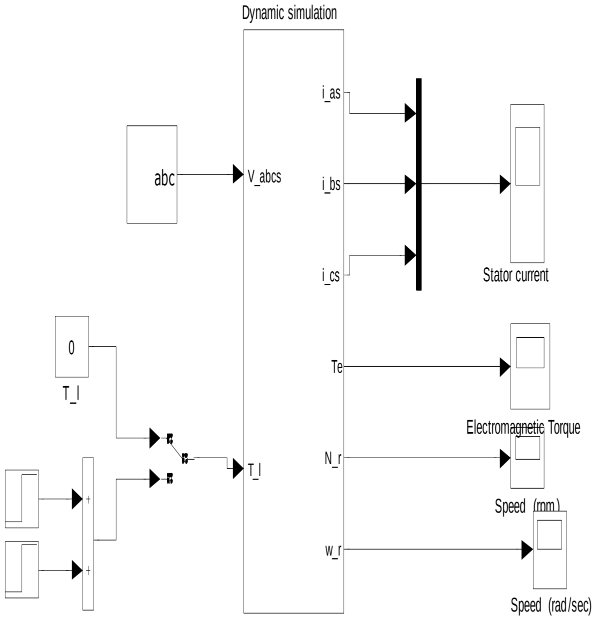

Fig. 2: The Complete Simulink Model of the 3-Phase IM Model.

4. MATLAB/Simulink sub system

A subsystem is a set of blocks that is replaced with a single subsystem block. As the model increases in size and complexity, it can be simplified by grouping blocks into subsystems. As it is built there is a kind of established hierarchical order, where a Subsystem block is on one level and the blocks that make up the subsystem are on another level. It has the advantage of keeping functionally related blocks together and ultimately reduces the number of blocks displayed in the model window. The sub-models of the equations used in the complete Simulink model are shown below:

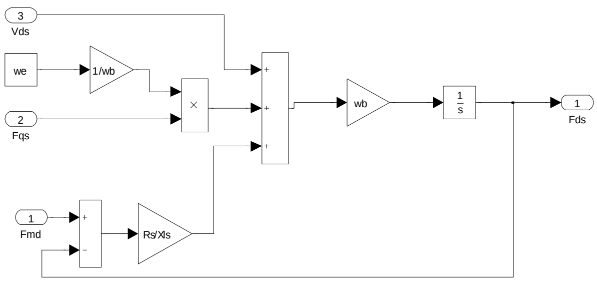

Fig. 3: A) Sub-Model of Equations (5).

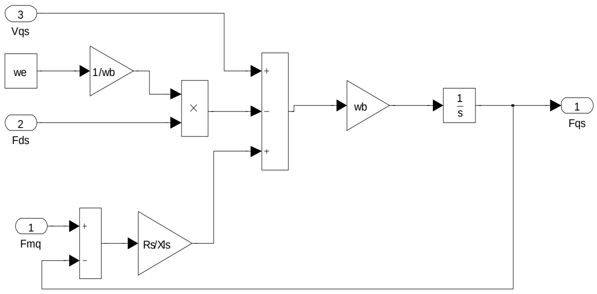

Fig. 3: B) Sub-Model of Equations (6).

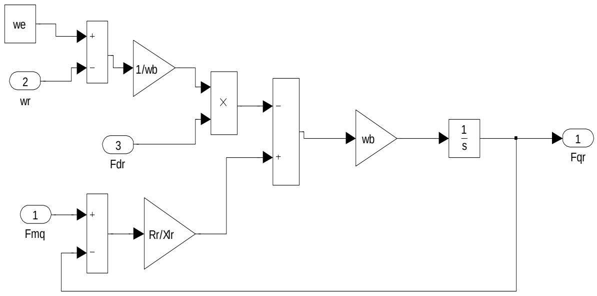

Fig. 3: C) Sub-Model of Equations (7)

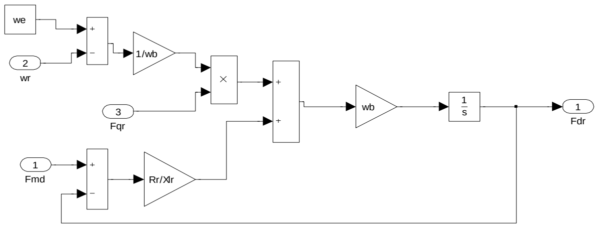

Fig. 3: D) Sub-Model of Equations (8).

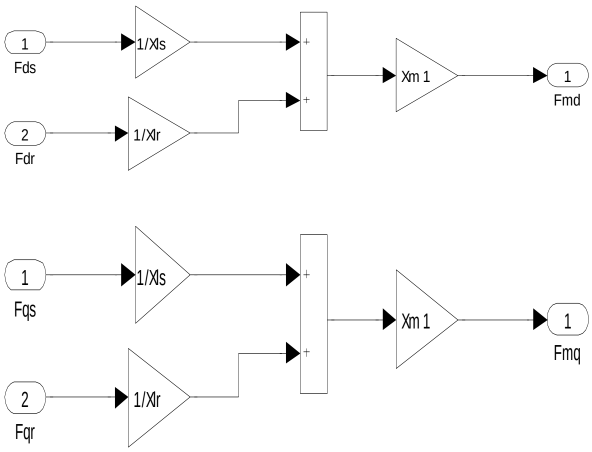

Fig. 4: Sub-Models of Equations (9) and (10).

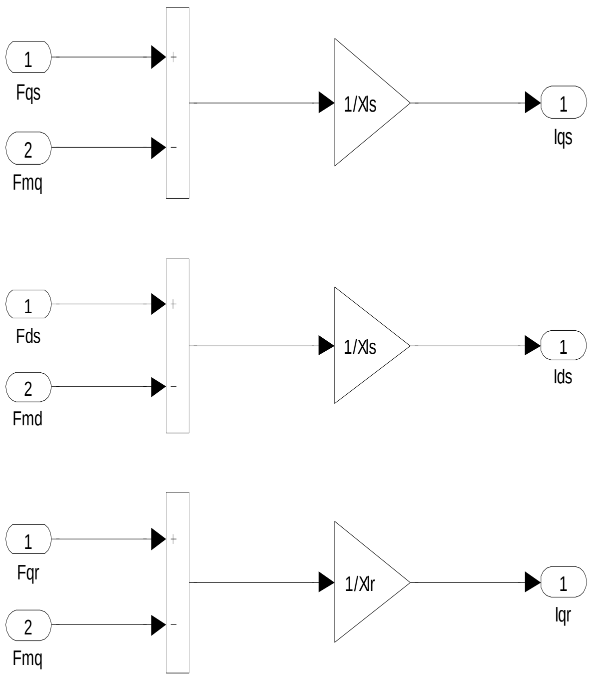

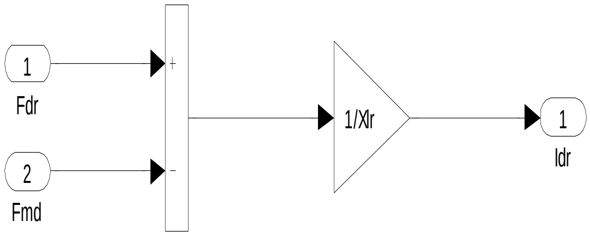

Fig. 5: Sub-Models of Equations (11) – (14).

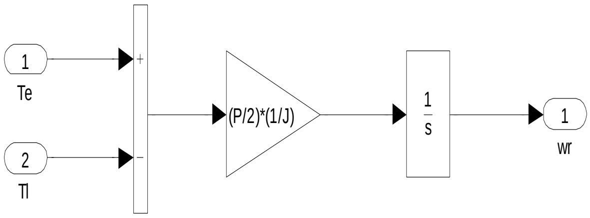

Fig. 6: Sub-Model of Equation (16).

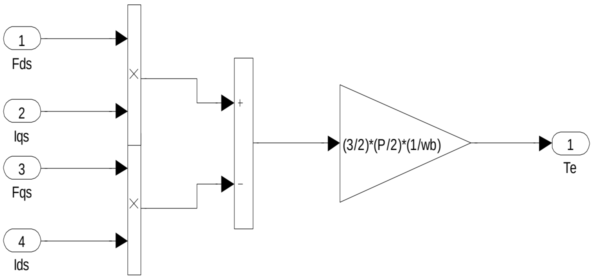

Fig. 7: Sub-Model of Equation (15).

5. Analysis of the simulation results

In table 1, the parameters of the motor are presented followed by the graphical representation used for the analyses.

Table 1: Parameter for the Three Phase Squirrel Cage Induction Motor [7], [17]

Parameters	Values
Rated Power	10Hp
Rated Line Voltage	400V
Supply Frequency	50Hz
Rated Speed	1440rpm
Inertia	0.0343Kg.m^2
Number of Poles	4
Stator Resistance	0.7384Ω
Rotor Resistance	0.7402 Ω
Rotor Inductance	3.045mH
Mutual Inductance	0.1241H
Stator Inductance	3.045mH

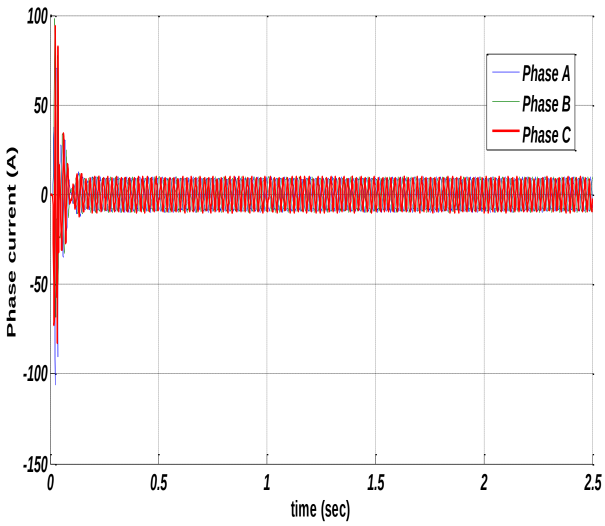

Fig. 8: Phase Current Against Time at No-Load.

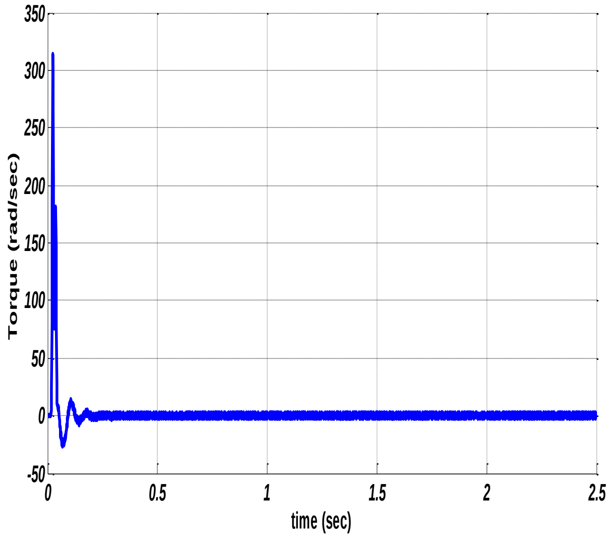

Fig. 9: Torque Against Time at No-Load.

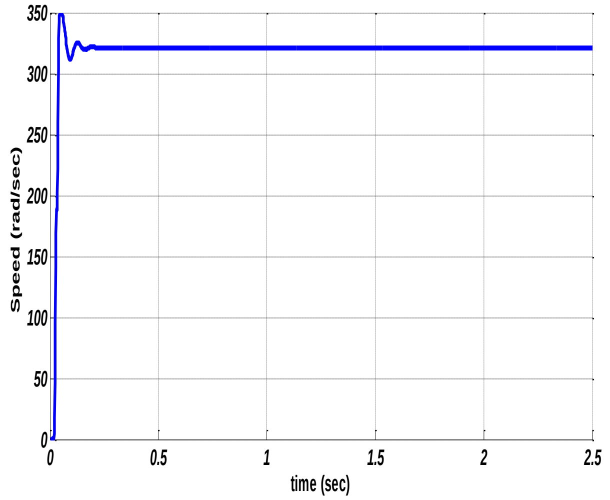

Fig. 10: Speed Against Time at No-Load.

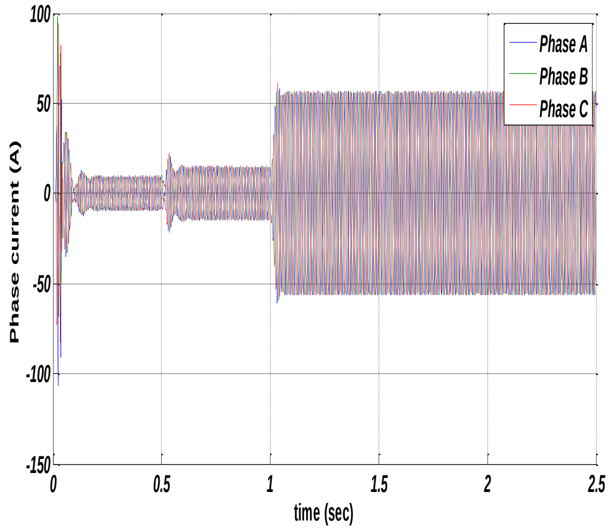

Fig. 11: Phase Current Against Time When Driving Load.

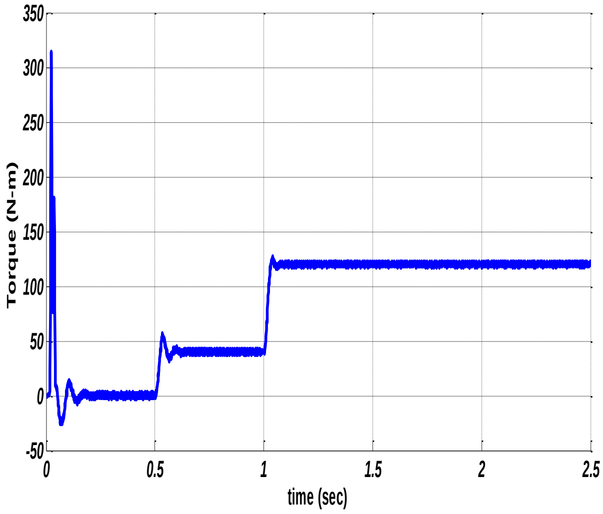

Fig. 12: Torque Against Time When Driving Load.

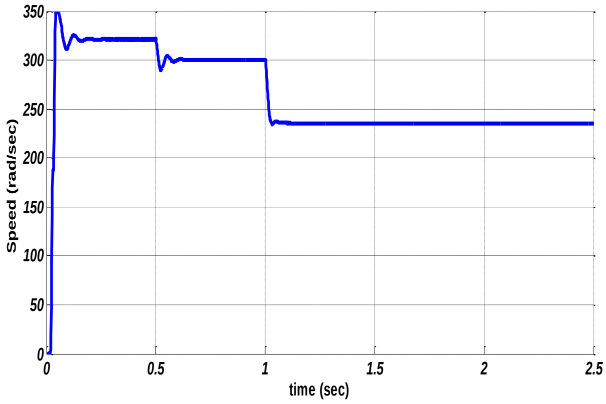

Fig. 13: Speed Against Time When Driving Load.

With the application of the rated voltage, the current, torque and speed increases to a very high value (as shown in Figures 8, 9 and 10 respectively) and eventually returns to its rated values. This increase may be as a result of disturbances in the power lines and it is the drawback of direct-on-line starting of the induction motor. Therefore, it is advisable to use a reduced voltage method of starting such as star-delta, auto-transformer method, etc. to reduce these high values during starting [3]. In Figure 11 specifically, as the motor is loaded, the tendency of the motor to respond to the loading will be such that more inertia will be exerted for the system to continue. At 0.12s, the associated high current or surge dropped giving rise to steady state. However, the cases of Figure 11 and Figure 8 are different. The high current shows that more work is done when the load is introduced than when it is not experiencing external load. From Figure 10 and Figure 13, there is this attendant reduction in speed with the introduction of load. From Figure11, when a variable load is applied, the phase current increases from 25A at 40N-m to 52A at 80N-m, the torque in Figure 12 also increases from 46N-m at 40N-m to 120N-m at 80N-m but in Figure 13, the speed decreases from 300rad/sec at 40N-m to 245rad/sec at 80N-m.

6. Conclusion

This work has presented the performance of the 10hp squirrel cage induction motor in response to the driven variable load. In terms of the electromagnetic torque and rotor speed behaviors, the model which was simulated at no-load and at variable loads of 40N-m and 80N-m, gave satisfactory responses. It was found that at the initial stage of load introduction, the machine is capable of attempts to adjust to new load-ability condition. With the proper incorporation of power semi-conductor devices, a better response is to be expected. The results obtained would indeed provide vital information to the motor manufacturers, Plant Electrical Engineers and Engineering researchers on the motor performance with respect to its design.

References

[1] S.E. Oti, C.A. Nwosu and D.B. Nnadi, Dynamics and Performance Characteristics of a 5hp Induction Machine, *Elixir International Journal, Electrical Engineering. 115 (2018), pp. 49686-49689.*

[2] C.U. Ogbuka, "Dynamic Modeling and Simulation of a 3-HP *Asynchronous Motor Driving a Mechanical Load*", Department of Electrical Engineering, University of Nigeria, Nsukka.

[3] S. E. Oti, C.A. Nwosu, D.B. Nnadi Damian, V. Madueme , Simulating performance characteristics of induction motor under a balanced load by direct on-line starting, *International Journal of Engineering &Technology, 7 (4) (2018) 6851-6855, doi: 10.14419/ijet.v7i4.27100.*

[4] A.A. Ansari and D.M. Desphande, "*Mathematical Model of Asynchronous Machine in MATLAB SIMULINK*", International Journal Engineering Science and Technology", Vol. 2(5), 2010, pp. 1260-1267.

[5] S. Gupta and Dr. S. Walhwani, "*Dynamic Modeling of Induction Motor Using Rotor Rotating Reference Frame*", International Journal of Advance Research in Electrical, Electronics and Instrumentation Engineering, Vol. 3, Issue 6, June 2014.

[6] S.E. Oti, C. A. Nwosu, D.B. Nnadi and O.I. Okoro, Performance study of three-phase induction motor driving a load, *Discovery*, 2019, 55(282), pp. 279-290.

[7] S.E. Oti, Thermal modelling of Induction Machine using the Lumped Parameter Model, Doctorate Degree Thesis, University of Nigeria, Nsukka, December 2014, pp. 1-140.
[8] A. Aktaibi and D. Ghanim, "*Dynamic Simulation of a Three Phase Induction Motor Using Matlab Simulink*", Faculty of Engineering and Applied Science, Memorial University of Newfoundland St. John's NL, Canada, AIB3X5.
[9] Oti S.E, Akpama E.J. Nnadi D. B., Performance Characteristic of Induction Motor under a Balanced Load by Star-Delta Starting: International Journal of Engineering and Management Research (IJEMR), Vol. 6, Issue 1, January-February 2016, pp. 30-34.
[10] O.I. Okoro, Steady State and Transient Analysis of Induction Motor Driving a Pump Load, Nigerian Journal of Technology, NIJOTECH, Vol. 22, No. 1, March 2003, pp.46-53.
[11] https://www.shodhganga.inflibnet.ac.in//11_chapter3/Dynamic_modelling_of_induction_motor. Retrieved on April 2017.
[12] H. L. Stewart, Pumps, Indianapolis: Sams, 1977, pp. 465.
[13] A. A. Divona and A. J. Dolan, "Electric motors and motor controls," In: Karassik, I. J., Krutzsch, W. C., Fraser, W. H. and Messina, J. P. (Eds.), Pump Handbook, pp. 6.3–6.25, NY: McGraw Book Company, 1985.
[14] B. K. Bose, Modern Power Electronics and AC Drives, Englewood Cliffs, NJ: Prentice-Hall PTR, 2001.
[15] V. Vodovozov and I. Bakman, Performance Improvement of Pumps Fed by the Variable Speed Drives, Electrical, Control and Communication Engineering ,2013 / 4 45, doi: 10.2478/ecce-2013-0021. https://doi.org/10.2478/ecce-2013-0021.
[16] P.B. Deb and S. Sarker, "*Dynamic Model Analysis of Three Phase Induction Motor Using Matlab/Simulink*", International Journal of Scientific and Engineering Research, Vol. 7, issue 3, March 2016.
[17] Krause, P.C., O. Wasynczuk, and S.D. Sudhoff, Analysis of Electric Machinery, IEEE Press, 2002. https://doi.org/10.1109/9780470544167.